Renewable and Sustainable Energy Reviews 96 (2018) 487–501

Contents lists available at ScienceDirect

Renewable and Sustainable Energy Reviews

journal homepage: www.elsevier.com/locate/rser

A novel integrated framework to evaluate greenhouse energy demand and crop yield production

Farzin Golzar[a,b], Niko Heeren[a,*], Stefanie Hellweg[a], Ramin Roshandel[b]

[a] Institute of Environmental Engineering, ETH Zurich, Zurich, Switzerland
[b] Department of Energy Engineering, Sharif University of Technology, Tehran, Iran

A R T I C L E I N F O

Keywords:
Greenhouse
Energy demand
Crop yield model
Integrated framework
Dynamic modeling

A B S T R A C T

Greenhouses are complex systems that require considerable amounts of energy. In order to optimize their performance, it is necessary to reduce the amount of energy per unit of crop produced. This requires a combined assessment of greenhouse energy balance and crop growth, as well as their interaction. In this work, more than 30 existing greenhouse models are reviewed and different algorithms are combined to propose an integrated energy-yield model. The physical model of greenhouse energy demand is based on the dynamic energy and mass balance while yield production is based on a physiological crop model.

The integrated model is validated with observed energy demand and crop yield datasets during one full tomato growing period. There was good agreement between modeled results and measured data. The key advantage of the integrated model is that it can analyze drivers for greenhouse energy losses and quantify the influence of measures on both energy demand and crop yield. Due to the model's dynamic and high temporal resolution, it is possible to study the use of renewable energy sources in greenhouse operation, as illustrated for thermal storage by means of phase change materials. A sensitivity analysis by changing day/night temperature, CO_2 indoor concentration and artificial lighting is performed. The results illustrate how the model can be used for optimizing the performance of greenhouses in terms of specific energy demand (energy per crop produced). Therefore, the integrated model can be a tool for determining the optimum design and control parameters, which is particularly relevant for growers and sustainable agriculture systems in general. This study presents a parametric decision support tool that assists planers with optimizing energy performance of greenhouses while analyzing the trade-off between energy demand and crop yield.

1. Introduction

In light of the growing worldwide population, efficiency increases in agricultural production are needed to meet the additional food demand. Food production by means of greenhouses represents a strategy to increase crop yields, by providing favorable ambient conditions of temperature, water supply and fertilization with CO_2 and nutrients [1]. This allows to prolong the cultivation period in cold regions and therefore also to avoid environmental impacts for food transport. However, providing a favorable climate in the greenhouse, especially during offseason cultivation of crops, requires more energy consumption than open field agriculture [2,3]. Therefore, increasing protected cultivation in greenhouses to achieve more yield per unit area will increase the energy consumption [4–7] and related environmental impacts [8–11], making the specific energy demand (i.e. units of energy per crop yield) of greenhouses a crucial issue [12,13]. For instance, production costs in EU greenhouses, as the largest supplier of greenhouse products, is 78% of total cost, with energy consumption being the largest share [14–17]. By shifting towards renewable energies for greenhouse operation, it is possible to reduce non-renewable energy consumption by 40% [14,16]. Hassanien et al. [18] review the utility of solar energy technologies in the greenhouse microclimate control systems specifically heating, cooling, lighting and irrigation systems. They show that advanced solar energy technologies such as solar air heaters, solar thermal collectors and photovoltaic (PV) water pumping can usually be applied very well in greenhouse and thus reduce environmental impact. Gül Bayrakci et al. [19] quantify the potentials of renewable energy sources, such as solar, biomass, wind, geothermal, and hydropower for Turkey. Greenhouses can be considered the largest commercial solar buildings [20], as they use solar energy to allow cultivation of different crops in places where previously no agriculture was possible [21].

* Corresponding author.
E-mail address: nheeren@ethz.ch (N. Heeren).

https://doi.org/10.1016/j.rser.2018.06.046
Received 1 November 2017; Received in revised form 20 April 2018; Accepted 20 June 2018
Available online 29 August 2018
1364-0321/

Nomenclature

Symbols

C_a	Specific heat of air ($J\,kg^{-1}\,K^{-1}$)
C	Condensation on the greenhouse cover, [$g\,m^{-2}\,s^{-1}$]
C_{CO2}	CO_2 concentration of inside greenhouse (ppm)
$D_F(T_d)$	Function for fruit development rate (day^{-1})
E	Crop transpiration ($g\,m^{-2}\,s^{-1}$)
$f_F(T_d)$	Function to modify partitioning to fruit vs. Average daily temperature, T_d (dimensionless)
$f_N(T)$	Function to modify node development rate as a function of hourly temperature (dimensionless)
GR_{net}	Net aboveground growth rate (g dry weight m^{-2} ground day^{-1})
h	the average height of the greenhouse (m)
LAI	Leaf Area Index (m^2 leaf m^{-2} ground)
LAI_{max}	Maximum leaf area index (m^2 leaf m^{-2} ground)
N	Number of nodes on main stem
N_b	Coefficient in expolinear equation, projection of linear segment of LAI vs N to horizontal axis (node)
N_{FF}	Nodes per plant when first fruit appears (node)
N_m	Maximum rate of node appearance rate per hour at optimal temperature (node h^{-1})
p_1	Loss of leaf dry weight per node after LAI_{MAX} is reached (g leaf $node^{-1}$)
$PPFD$	Photosynthetic photon flux density ($\mu mol\,m^{-2}\,s^{-1}$)
q_{con}	the convective and conductive heat transfer (W)
q_g	The input energy to maintain the desired temperature in the greenhouse (W)
q_l	The energy exchange of the thermal radiation from the greenhouse interior to outside (W)
q_{lamp}	Energy transfer of artificial lighting (W)
q_{trans}	the heat flux due to crop transpiration (W)
q_{solar}	The energy transfer of incoming solar radiation (W)
q_{vent}	Heat loss due to natural ventilation (W)
T	Hourly temperature (°C)
T_d	Average daily temperature (°C)
$T_{daytime}$	Average temperature during daytime hours (°C)
V_a	greenhouse volume (m^3)
V	Moisture loss through the ventilation windows, [$g\,m^{-2}\,s^{-1}$]
W	Above ground dry weight (g dry weight m^{-2} ground)
W_F	Total fruit dry weight (g dry weight m^{-2} ground)
W_M	Mature fruit dry weight (g dry weight m^{-2} ground)

Greek symbols

α_F	Maximum partitioning of new growth to fruit (fraction day^{-1})
β	Thermal expansion coefficient (dimensionless)
β_C	Coefficient in expolinear equation ($node^{-1}$)
δ	Maximum leaf area expansion per node (m^2 leaf $node^{-1}$)
κ_F	Development time from first fruit to first ripe fruit (node)
$\lambda(T_d)$	Temperature function to reduce rate of leaf area expansion (dimensionless)
υ	Transition coefficient between vegetative and full fruit growth ($node^{-1}$)
ρ	Plant density (number of plants m^{-2} ground)
ρ_a	greenhouse air density ($kg\,m^{-3}$)
ϕ_{CO2}	CO_2 flux ($g\,m^{-2}\,s^{-1}$)
χ	Absolute water vapour concentration of greenhouse air, [$g\,m^{-3}$]
ψ	Roof slope (degree)

Subscripts

O	Outdoor condition
$crop$	Crop level
air,sat	Saturated air

Protected cultivation systems can be found around the world. They range from passive solar greenhouses [22,23] and low-cost greenhouses [24–29] to the high-tech greenhouses [7,30]. There is a trend towards more use of renewable energy technologies, such as PV modules, solar thermal collectors and thermal energy storages, to decrease fossil fuel consumption of conventional greenhouses [4,31,32]. Cuce et al. [31] concluded that 80% energy saving in greenhouses is achievable by appropriate application of renewable energy resources depending on climatic conditions and crop type. To consider the impact of them on the greenhouse energy consumption and yield production for designing an optimum energy system, an integrated model is required to investigate both issues, simultaneously. Such an integrated model is missing in literature, as previous models have focused on either energy demand or crop growth. Such an integrated model is missing in literature, as previous models have focused on either energy demand or crop growth.

1.1. Greenhouse energy models

Typical numerical energy demand models for buildings are not suitable for determining energy demand of greenhouses. The main reason for this is the microclimate in the greenhouse, which is determined by the crop canopy during different stages of crop growth, is constantly changing, unlike typical buildings [33]. A number of authors have developed approaches to determine greenhouse specific energy demand. Following an initial analysis of greenhouse energy balance to simulate greenhouse inside temperature [34,35], a number of dynamic models were developed. These models simulate the greenhouse climate as a function of the outdoor climate and the greenhouse's physical features [36–39]. Tiwari et al. [40], Chou et al. [41] and Singh et al. [27] used previously developed dynamic models as an analytical model to estimate energy demand by considering the impacts of different sizes and shapes of greenhouses. Sethi et al. [42] improved the previous dynamic energy models by modeling the effects of solar radiation on different greenhouse shapes. Vanthoor et al. [43] extended the model of Bot [38] and developed a greenhouse climate model to apply to four different greenhouse designs under three climatic conditions. Vadiee and Martin [20] investigated the performance of the closed greenhouses with long or/and short thermal storage technology (TES) integration. Van Beveren et al. [30] and Joudi and Farhan [26] developed and validated dynamic greenhouse microclimate models to describe the energy and mass exchanges between the inside and outside of the greenhouse, and applied the models to analyze the thermal performance in the greenhouses. Chen et al. [33] proposed a methodology to predict the energy demand of greenhouses based on the energy and mass balance. They utilized a sensitivity analysis methodology to calibrate the uncertain parameters of the energy model by using the measured data in an experimental greenhouse. Although some of the abovementioned energy models consider different basic greenhouse energy losses, none of them is able to directly account for the effects of plant growth, namely evapotranspiration with dynamic leaf area index and CO_2 assimilation. While they use some parameters from crop type as inputs, they cannot predict the impact on yield production.

Table 1
Overview of existing greenhouse models in chronological order of publication date and list of terms and processes considered. n/a denotes that the authors did not include the term. LAI: Daily calculated Leaf Area Index production (not as an average constant parameter) is considered.

Reference	Energy model			Crop model			Description
	Indoor Temperature	Indoor CO_2	Indoor Humidity	LAI	Photosynthesis	Yield	
Businger, 1963 [35]	Dynamic energy balance	n/a	n/a	n/a	n/a	n/a	Simulation of greenhouse inside temperature with good precision but complex and not easy to use for long periods
Walker, 1965 [34]							
Takakura et al., 1971 [36]	Dynamic energy balance	Dynamic CO_2 balance	n/a	n/a	CO_2 assimilation	n/a	Improved dynamic model and included the heat storage in the soil
Van Bavel et al, 1981 [37]	Dynamic energy balance	Dynamic CO_2 balance	Dynamic humidity balance	n/a	n/a	n/a	Simulation of the greenhouse climate as a function of the outdoor climate and the greenhouse's physical features
Bot, 1983 [38]							
Deltour et al, 1985 [39]							
Nederhoff et al., 1993 [57]	n/a	Dynamic CO_2 balance	n/a	n/a	Rate of net photosynthesis	n/a	Effect of various CO_2 concentration on tomato, cucumber and sweet paper growth
De Zwart, 1996 [58]	Dynamic energy balance	Dynamic CO_2 balance	Dynamic humidity balance	n/a	n/a	n/a	Simulation model to study energy-saving options Natural ventilation heat loss is used in our model in an adapted form. (See Supporting Information, Section 1.1 and Eqs. S.15 to S.21).
Tiwari, 1998 [40]	Instantaneous thermal efficiency	n/a	n/a	n/a	n/a	n/a	Expression for thermal efficiency of a greenhouse in terms of design and climatic parameters
Kempkes et al., 1998 [59]	Crop temperature distribution	n/a	n/a	n/a	n/a	n/a	Vertical temperature distribution of a greenhouse crop description
Heuvelink, 1995, 1996, 1999 [45-47]	n/a	n/a	n/a	n/a	n/a	Dry matter production	Dynamic simulation model for tomato crop growth and development
Sharma, 1999 [60]	Dynamic energy balance	n/a	n/a	n/a	n/a	n/a	Determination of plant and the enclosed room air temperature in different zones of the micro-climate of a greenhouse
Wang et al., 1999 [61]	Dynamic energy balance	n/a	Observed relative humidity	n/a	n/a	n/a	Experimental regression model for predicting the global vegetation temperature
Jones et al., 1991, 1999 [49, 50]	n/a	n/a	n/a	Hourly LAI production	Hourly Carbohydrate production	Daily fruit production	Development of a dynamic tomato growth and yield model LAI, photosynthesis and yield production models are used in our model in an adapted form. (See Section 2.2 and Eqs. 4 to 8).
Abreu et al., 2000 [48]	n/a	n/a	n/a	n/a	n/a	Weekly fruit production	Simulation of the weekly production of greenhouse tomatoes
Trigui et al., 2001 [62, 63]	Dynamic energy balance	Dynamic CO_2 balance	Dynamic humidity balance	n/a	Carbohydrate production rate	n/a	Prediction the dynamic ambient greenhouse air conditions maximizing a tomato crop yield
Ramirez et al., 2004 [52]	n/a	n/a	n/a	LAI production	Carbohydrate production	Fruit production	Comparison the more complex model of TOMSIM and simplified version of TOMGRO Some constant parameters of TOMGRO from this work. (See Supporting Information, Table S.1)
Chou et al., 2004 [41]	Dynamic energy balance	n/a	Dynamic humidity balance	n/a	n/a	n/a	Study the performance of heat pump to meet the heating and dehumidification requirements
Singh et al., 2006 [27]	Dynamic energy balance	n/a	n/a	n/a	n/a	n/a	Four components temperature of the greenhouse cover, inside air, canopy surface and bare soil surface
Bontsema et al., 2007 [64]	n/a	n/a	Dynamic humidity balance	n/a	n/a	n/a	Estimation of on-line transpiration of a crop in a greenhouse Transpiration modeling is used in our model in an adapted form. (See Supporting Information, Section 1.1, Eqs. S.9 to S.14)
Dimokas, 2008 [55]	n/a	n/a	n/a	Hourly LAI production	Hourly Carbohydrate production	Daily fruit production	Application of TOMGRO for different geographical locations
Sethi, 2009 [42]	Dynamic energy balance	n/a	n/a	n/a	n/a	n/a	Modeling the effects of solar radiation on different greenhouse shapes and review of thermal models
Vanthoor, 2011 [43]	Dynamic energy balance	Dynamic CO_2 balance	Dynamic humidity balance	n/a	n/a	n/a	Development a model- based method to design greenhouses for a broad range of climatic and economic conditions
Vanthoor, 2011 [44]	n/a	n/a	n/a	n/a	Carbohydrate production	Fruit production	Description and validation of the effects of greenhouse climate on yield

(*continued on next page*)

Table 1 (*continued*)

Reference	Energy model			Crop model			Description
	Indoor Temperature	Indoor CO_2	Indoor Humidity	LAI	Photosynthesis	Yield	
Vanthoor, 2011 [12]	Dynamic energy balance	Dynamic CO_2 balance	Dynamic humidity balance	LAI production	Carbohydrate production	Fruit production	Sensitivity analysis of a combined greenhouse climate -crop yield model of tomato
Bacci et al., 2012 [54]	n/a	n/a	n/a	Hourly LAI production	Hourly Carbohydrate production	Daily fruit production	Application of TOMGRO for different geographical locations
Sethi, 2013 [65]	Thermal modeling	n/a	n/a	n/a	n/a	n/a	A review on heating technologies We used the generalized procedure for developing greenhouse thermal Model. (See Section 2.1)
Vadiee and martin, 2013 [20]	Dynamic energy balance	n/a	n/a	n/a	n/a	n/a	Performance investigation of the closed greenhouses with long or/and short thermal storage technology (TES) integration
Van Beveren et al., 2015 [30]	Dynamic energy balance	Dynamic CO_2 balance	Dynamic humidity balance	n/a	n/a	n/a	A dynamic optimization tool development based on optimal control theory CO_2 and relative humidity balances are used in our model in an adapted form. (See Section 2.1 and Eqs. 2 and 3.
Joudi and Farhan, 2015 [26]	Dynamic energy balance	n/a	n/a	n/a	n/a	n/a	Development and validation dynamic greenhouse microclimate
Chen et al, 2016 [33]	Dynamic energy balance	n/a	n/a	n/a	n/a	n/a	Prediction the energy demand of greenhouses based on the energy and mass balance Energy balance is used in our model in an adapted form. (See Section 2.1 and Eq. 1).
Shamshiri et al., 2016 [56]	n/a	n/a	n/a	Hourly LAI production	Hourly Carbohydrate production	Daily fruit production	Application of TOMGRO for different geographical locations

1.2. Greenhouse crop yield models

A number of vegetable crop models, which investigate the effect of greenhouse climate conditions on crop growth and yield, are discussed in the literature [44]. Some of the more common models for tomato yield are TOMSIM (Heuvelink [45–47]), TOMPOUSSE (Abreu et al. [48]) and TOMGRO (Jones et al. [49,50]). TOMPOUSSE is a simple model to estimate weekly production of greenhouse tomatoes [48]. This model investigates the effect of the weekly average greenhouse air temperature on flowering rate and harvested fruits by a linear regression model. TOMSIM and TOMGRO have been developed based on dry matter production and dry matter distribution. Both of these models use the same approach for dry matter production. Potential crop growth rate is computed by integration of hourly leaf assimilation rates over total crop leaf area throughout the day. Crop growth is resulted by multiplying the conversion efficiency. Differences between these two models are due to dry matter partitioning and interactions between dry matter production and partitioning. Both of these models are able to account for the effects of temperature, CO_2 concentration and solar radiation on crop yields. The TOMGRO model comes in various versions of differing complexity. The original model [49] has 69 state variables, an advanced version of the model has 574 state variables [51] and, finally, a simplified version has only five state variables [50]. The results of Jones et al. [50] showed that the simplified version of TOMGRO is sufficient in predicting tomato growth and yield for different locations. Ramirez et al. [52] compared the more complex model of TOMSIM and simplified version of TOMGRO for total dry matter production in greenhouses located in Southeast of Spain. The difference between both models is that TOMGRO calculates leaf area index and TOMSIM computes the number of fruit trusses as the vegetative development rate. Ramirez et al. [52] and Bertin and Heuvelink [53] showed that both models can represent the dynamic growth behavior of a tomato crop with varying numbers of input variables. Several works [54–56] confirmed the application of the reduced state variables version of TOMGRO for different geographical locations, such as Italy, Greece, and Malaysia. All of the articles conclude that crop models are useful for investigating the effects of greenhouse microclimate on crop growth and yield. However, none of them are capable of quantifying the amount of energy which is needed to provide favorable climate conditions.

1.3. Coupling of greenhouse and crop yield models

Table 1 summarizes and characterizes the most important models for simulating greenhouse energy demand and crop growth.

To our knowledge, the only model that includes a full energy and crop model and the related terms and processes listed in Table 1 was performed by Vanthoor et al. [12]. However, their model uses the estimated indoor climate (energy, CO_2 and humidity) as input for the tomato yield model, but does not consider feedback influence of crop growth on indoor climate. Therefore, their model only can investigate the effects of indoor climate on yield production (e.g. effect of indoor CO_2 concentration on crop yield) but would not be able to analyze the impacts of crop growth stages on greenhouse microclimate and energy demand (e.g. impact of LAI expansion on heat loss). Other than that, no integrated framework considering all important terms in greenhouse energy demand and crop growth, and therefore their mutual effects, exists.

Only an integrated model can account for every stage of crop growth in different seasons and the effect on total energy consumption and yield production.

In this work a new integrated framework fulfilling the following requirements is proposed:

i) couple greenhouse energy demand and crop yield models and improve state-of-the-art of integrated greenhouse energy-crop yield

models
ii) perform integrated simulations of energy demand and crop growth on a high temporal resolution
iii) evaluate the integrated model with empirical data from existing greenhouses
iv) analyze the potential of renewable energy use
v) investigate the possible effects of different set points over practical ranges of temperature, CO_2 and light

To fulfill these requirements we combine the greenhouse energy and climate models by Chen et al. [33], Van Beveren et al. [30], Van Beveren et al. [7], De zwart [58] and Bontsema et al. [64] and formulate greenhouse model based on a generalized procedure which is introduced by Sethi et al. [65]. The reduced state variable of TOMGRO [50] is selected as the basis for the crop growth model. These models were selected because they take into account all basic energy demand and crop growth mechanisms in a dynamic way. The dynamic and comprehensive behavior of the selected models in their own fields helps us to develop the integrated model.

The proposed integrated framework simulates the energy balance within a climate-controlled greenhouse, focusing on heating energy demand. By calculation of greenhouse energy demand, decision makers (growers and greenhouse holders) would be able to design a new optimum energy supply systems or improve an old one.

2. Model description

Greenhouse climate is typically described by indoor temperature, humidity and CO_2 concentration [7]. For keeping each parameter in an acceptable range for crop growth, greenhouses require conditioning of the indoor climate, which requires energy for different kinds of processes (heating, cooling, ventilation, etc.) and materials (glazing, plastic cover, etc.).

2.1. Dynamic energy model

Energy gains and losses were quantified for individual time steps. In this work two kinds of time steps are considered: *a*) hourly time step which is demonstrated by *i* and varies from 1 to 24, *b*) daily time step which is represented by *j* and varies from 1 to 365. Although hourly time step has a higher temporal resolution in greenhouse energy demand, the daily time step for crop growth is needed for the sake of integration of energy-crop yield model.

The energy balance used in this work is based on Chen et al. [33]. This model simulates all important energy flow mechanisms as functions of inside air temperature. Therefore, by controlling inside air temperature, the greenhouse heating energy demand will be determined. We adapted the model so that heat flux due to crop transpiration and ventilation are calculated, as introduced in the models of Van Beveren et al. [30] and De Zwart [58], respectively. The enhanced overall greenhouse heat balance equation is presented in Eq. (1) [33]:

$$q_g(i,j) = \rho_a V_a C_a \frac{dT_{in}(i,j)}{dt_i} - [q_{solar}(i,j) + q_{lamp}(i,j)] + q_{con}\left(i,j\right) + \dots + q_{trans}(i,j) + q_l(i,j) + q_{vent}(i,j) \qquad i = 1, 2, \dots, 24 \qquad j = 1, 2, \dots, 365 \tag{1}$$

Where (*i,j*) is *i*th hour of *j*th day of year, q_g is the hourly energy required (model output) to maintain the desired temperature in the greenhouse (W), ρ_a is the indoor air density (kg m^{-3}), V_a is the total indoor air volume (m^3), C_a is the specific heat capacity of air (J kg^{-1} K^{-1}), T_{in} is hourly indoor desire temperature (model input), q_{solar} is the energy transfer of incoming solar radiation (W) in the interior (Eq. (S.2)), q_{lamp} is energy transfer of artificial lighting (W) (Eq. (S.3)), q_{con} is the convective and conductive heat transfer (W) (Eq. (S.5)), q_{trans} is the energy flux due to crop transpiration (W) (Eq.(S.9)), q_l is the energy exchange with the exterior due to long-wave and short-wave radiation (W) (Eq. (S.6)), and q_{vent} is the energy transfer due to mass transfer by means of ventilation (W) (Eq. (S.15)). The related equations to calculate all terms in Eq. (1) are explained in the Supporting Information through Eqs. (S.1) to (S.21). Also, parameter description and constant values are summarized in table (S.1).

The humidity balance for a greenhouse is described by [7,30,64]:

$$G_\chi(i,j) = h\frac{d\chi(i,j)}{dt_i} - E\left(i,j\right) + V\left(i,j\right) + C\left(i,j\right) \qquad i = 1, 2, \dots, 24 \qquad j = 1, 2, \dots, 365 \tag{2}$$

Where G_χ is the amount of water necessary to inject into or reject from the greenhouse for maintaining the desired water content in the greenhouse atmosphere (g m^{-2} s^{-1}), *h* is the average height of the greenhouse (m), *E* is the crop transpiration rate (g m^{-2} s^{-1}) (Eq. (S.23)), *V* is the moisture loss through ventilation (g m^{-2} s^{-1}) (natural and/or mechanical, Eq. (S.25) and *C* is the condensation on the indoor greenhouse cover (g m^{-2} s^{-1}) (Eq. (S.24)) and occurs when the cover temperature is below the dew point temperature of the air.

CO_2 can be supplied to the greenhouse through replacing inside air with fresh air. However, in cold seasons with lower ventilation, CO_2 consumption can be higher than the CO_2 influx. When inadequate CO_2 is available from fresh air alone, CO_2 injection is required. The additional CO_2 can also enhance crop yield [49].

The CO_2 model that is applied in this work is based on [7] and total CO_2 balance in the greenhouse is described by:

$$\varphi_{CO_2,inj}(i,j) = h\frac{dC_{CO_2}(i,j)}{dt_i} + \varphi_{CO_2,a}\left(i,j\right) + \varphi_{CO_2,v}\left(i,j\right) \qquad i = 1, 2, \dots, 24 \qquad j = 1, 2, \dots, 365 \tag{3}$$

Where $\phi_{CO2,inj}$ is the injection of pure industrial CO_2 to the greenhouse (g m^{-2} s^{-1}), $\phi_{CO2,a}$ is the assimilation of CO_2 by the crop (g m^{-2} s^{-1}) (Eq. (S.28)) and $\phi_{CO2,v}$ is the CO_2 exchange with outside air due to ventilation (g m^{-2} s^{-1}) (Eq. (S.29)).

2.2. Dynamic crop growth and yield model

The applied crop growth and yield model in this work is based on TOMGRO, which was originated and developed through [49,50,66–71]. Jones et al. [50] simplified TOMGRO to a reduced state variable model. They simulated basic crop growth processes such as photosynthesis, respiration and node development using five state variables. Plant development is described by *N* (node) and Leaf area index (LAI) (m^2 leaf m^{-2} ground) as node number and leaf area index, respectively. *W* (g dry weight m^{-2} ground) is the total plant dry weight and describes the vegetative tissue development. Total fruit dry weight and mature fruit dry weight are modeled by W_F (g dry weight m^{-2} ground) and W_M (g dry weight m^{-2} ground). In this work, plants are assumed to be well fertilized and watered [49]. The effect of CO_2 concentration on crop growth is added to the model of Jones et al. [50]. The governing equations for calculation of each state variable are presented below.

Node development rate is modeled as multiplication of node maximum appearance rate per hour by a function that considers the effect of non-optimal temperatures on node appearance rate. The equation of node development rate is presented by Eq. (4) [50,72]:

$$\frac{dN(i,j)}{dt_i} = N_m f_N(T(i,j)) \qquad i = 1, 2, \dots, 24 \quad j = 1, 2, \dots, 365 \tag{4}$$

Where N_m is maximum rate of node appearance rate per hour at optimal temperature (node hour^{-1}) and $f_N(T(i,j))$ is a function to modify node development rate as a function of hourly temperature (-).

Leaf area index (LAI) is a simultaneous function of node development rate and temperature, and is calculated as [50]:

$$\frac{d(LAI(i,j))}{dt_i} = \rho\delta\lambda(T)\frac{\exp[\beta c\,(N(i,j)-N_b)]}{1+\exp[\beta(N(i,j)-N_b)]}\frac{dN(i,j)}{dt_i} \quad if: \quad LAI\left(i,j\right) \le LAI_{\max}$$

$$\frac{d(LAI(i,j))}{dt_i} = 0 \quad if: \quad LAI\left(i,j\right) > LAI_{\max} \quad i = 1, 2, \ldots, 24 \quad j = 1, 2, \ldots, 365 \tag{5}$$

where ρ is plant density (number of plants m^{-2} ground), δ is maximum leaf area expansion per node (m^2 leaf $node^{-1}$), $\lambda(T)$ is temperature function to reduce rate of leaf area expansion (-), βc and N_b are coefficients in expo linear equation and LAI_{max} is the maximum possible leaf area index (m^2 leaf m^{-2} ground).

Total plant weight is calculated by subtracting leaf removal or senescence from net aboveground biomass growth rate [49,50]:

$$\left(\frac{dW(j)}{dt_j}\right)_{actual} = \min\left[GR_{net}(j) - p_1\rho\left(\frac{dN(j)}{dt_j}\right),\ \frac{dW_F(j)}{dt_j} + (V_{\max}-p_1)\rho\left(\frac{dN(j)}{dt_j}\right)\right] \quad j = 1, 2, \ldots, 365 \tag{6}$$

Where (*j*) is *j*th day of year, GR_{net} is above ground biomass growth rate (Eq. (S.32)), p_1 is loss of leaf dry weight per node after LAI_{MAX} is reached (g[leaf] $node^{-1}$), W_F is fruit dry matter (Eq. (7)) and V_{max} is maximum increase in vegetative tissue dry weight growth per node (g [dry weight] $node^{-1}$).

The fruit dry matter developing rate is calculated by Eq. (7) [50]:

$$\frac{dW_F(j)}{dt_j} = GR_{net}(j)\alpha_F f_F(T_d(j))[1-\exp(-\upsilon(N(j)-N_{FF}))]\times\ldots \times g(T_{daytime}(j)) \quad if: \quad N > N_{FF} \quad j = 1, 2, \ldots, 365 \tag{7}$$

Where α_F is maximum partitioning of new growth to fruit (fraction day^{-1}), $f_F(T_d(j))$ is a function to modify partitioning to fruit for average daily temperature, υ is the transition coefficient between vegetative and full fruit growth ($node^{-1}$), N_{FF} is nodes per plant when first fruit appears (node) and $T_{daytime}(j)$ is average temperature during daytime hours (°C). Daytime hours are determined based on estimation of sunrise and sunset which are function of day number and latitude of greenhouse location [73].

Jones et al. [50] introduced a lag for maturity of the first fruit and used a function developed by Marcelis and Koning [74] to compute the average development rate:

$$\frac{dW_M(j)}{dt_j} = D_F(T_d)(W_F(j)-W_M(j)) \quad if: \quad N > N_{FF}+\kappa_F \quad j = 1, 2, \ldots, 365 \tag{8}$$

In Eq. (8), $D_F(T_d)$ is a function for fruit development rate (day^{-1}) and κ_F is development time from first fruit to first ripe fruit (node).

Eqs. (4)–(8) are five equations which, when solved, result in five state variables for describing the tomato growth and yield model. Node development rate (*N*) (Eq. (4)) and leaf area index (*LAI*) (Eq. (5)) are solved hourly. Their values at the end of each day are used in Eqs. (6)–(8). Complete explanations for crop growth model details are described through Eqs. (S.30) to (S.39)

Outputs of the model are the hourly heating and cooling demand, hourly energy losses and gains, hourly required CO_2 for the aim of CO_2 enrichment, hourly required water for the aim of relative humidity, hourly crop vegetative growth, daily fruit development rate and daily mature fruit production. The overall model structure and the relationships of mathematical equations are illustrated in Fig. 1.

2.3. Solution strategy

The integration procedure of energy-crop yield model is demonstrated in Fig. 2. Physical properties of the greenhouse construction and materials, such as cover materials, shape, number and size of windows, geographical direction, etc. are the first inputs of the integrated model. These inputs affect both the energy and crop growth models. For instance, thicker cover materials have less energy loss but reduce the amount of available solar radiation, which influences plant growth. Environmental conditions such as solar radiation, outside temperature, humidity, CO_2 concentration, wind speed and direction are the most important inputs affecting energy demand of a greenhouse. Indoor desired temperature, humidity and CO_2 concentration and crop physiological properties are the other important model input variables.

By solving Eqs. (1)–(5), hourly values for greenhouse demands (energy, CO_2 and water) and crop vegetative part's development are calculated. These hourly calculated values are taken as inputs to the next hourly time step. Node development (N) and leaf area index (LAI) values at end of each day are used as inputs of Eqs. (6), (7) and (8). Therefore, all state variables are refreshed hourly and daily. The advantage of this integrated model is that it can consider the effects of outside environmental conditions on energy demand and crop growth and their interactions at the same time. This feature of the model provides a powerful tool to optimize economic and environmental performance of the greenhouse.

2.4. Model validation with empirical data

The greenhouse empirical data belongs to Agroscope, a federal research institute in Conthey (46.2245°N, 7.3035°E), Switzerland. The tomato crop trial was conducted in a multi span Venlo type greenhouse of 12.8 m length, 28 m width and a 5 m average height for each compartment. The south wall is made of polycarbonate, the other ones are single glass and the roof is made of tempered security glass with a thickness of 4 mm. CO_2 was injected during the day until ventilation windows were 10% opened. The planting density was 3.47 stems per m^2. The operation period of the greenhouse was from 25.01.2016 to 12.10.2016. Hourly outdoor radiation, temperature, humidity, CO_2 concentration, and opening percent of thermal and shading screen were logged and are used as model inputs. General physical features of the greenhouse and operating set points are summarized in Table 2.

Model performance is investigated using quantitative techniques, which are divided into three major categories: standard regression, dimensionless techniques and error index. In this study, the coefficient of determination (R^2), relative root mean square error (*RRMSE*) and percent bias (*PBIAS*) are selected as representative of each category, respectively. The coefficient of determination (R^2), which is calculated using Eq. (S.40), determines the degree of linear relationship between simulated and measured data. R^2 ranges from 0 to 1, with higher values indicating less error variance. Values greater than 0.5 are considered acceptable [75]. Percent bias (*PBIAS*) evaluates the average tendency of the simulated data to overestimate or underestimate the reality [76]. Positive values present model underestimation bias, and negative values present model overestimation bias [77]. PBIAS is calculated with Eq. (S.41). Relative Root Mean Square Error (*RRMSE*) provides a relative model evaluation assessment and ranges between 0 and 1, with $RRMSE = 0$ being the optimal value and with lower values indicating less error [78]. Relative Root Mean Square Error (*RRMSE*) is calculated with Eq. (S.42):

3. Results

3.1. Model application and validation

To evaluate the overall integrated model performance, the modeled results are compared with observed data from the Agroscope greenhouse (described in Section 2.4). The hourly environmental climate condition data, greenhouse physical properties and agricultural management during crop growth are used as inputs of the integrated model. We compare the model results with empirical monthly energy consumption data, weekly yield data and annual energy consumption for 1 m^2 of greenhouse and 1 kg of yield.

Fig. 3 compares simulated energy consumption with observed data from Agroscope. As expected, energy demand reaches its maximum during the winter season. The integrated model estimates both winter and summer heating demand, which suggests that the model is capable of estimating energy demand during different seasons based on outdoor climate condition and crop growth. Greenhouse energy demand is decreased during spring, reached its lowest value in summer, and follows an increasing trend in the fall. The integrated model reflects this trend. An R^2 value of 0.91 indicates a highly linear relationship between observed and simulated data. An RRMSE value of 0.27 indicates an acceptable deviation of simulated data from observed data. A PBIAS value of 0.18 suggests an underestimation of the integrated model. While model can calculate the hourly heating demand, an aggregation to monthly heating demand was performed to compare these values with monthly observed data.

Different energy gains and losses are depicted in Fig. 4 to analyze the effects of heat transfer mechanisms on greenhouse energy demand. This figure highlights the role of the leaf area index on the transpiration heat losses. Losses are negligible in winter due to a low leaf area index at the beginning of the crop growth period. Other heat losses (such as conduction and convection heat losses from greenhouse cover and natural ventilation loss), are the dominant mechanisms for heat loss during that time due to high difference between greenhouse climate conditions and environmental conditions. Due to the increasing crop vegetative tissue (i.e. increased *LAI*) over time, the effect of transpiration loss on energy demand becomes more pronounced. During summer the leaf area index and solar radiation are at their maximum values, and transpiration loss becomes the second most important energy loss. Although solar energy gain is increased in summer, it causes more photosynthesis due to higher leaf area index and, consequently, also more transpiration loss.

Due to the large temperature difference between the indoor and exterior climates, natural ventilation is the most important source of energy loss during winter. As the growing season progresses, outdoor temperature and solar gains increase and it is necessary to increasingly evacuate warm air accumulated during the day by means of active cooling or mechanical ventilation to ensure favorable indoor conditions. Therefore, heat evacuation becomes the largest negative energy flow during summer. The model quantifies the accumulated excess heat, but does not consider the method of heat evacuation (e.g. active cooling or mechanical ventilation). While the focus of this work lies on modeling the demand side, supply technologies can be easily added in future work.

Fig. 5 illustrates simulated transpiration loss with and without considering feedback from crop growth. For simulating transpiration loss without crop growth feedback, an average value for leaf area index (LAI) is considered in the greenhouse energy model [7,30,33,64]. In this case, transpiration loss is a function only of solar radiation. Fig. 5

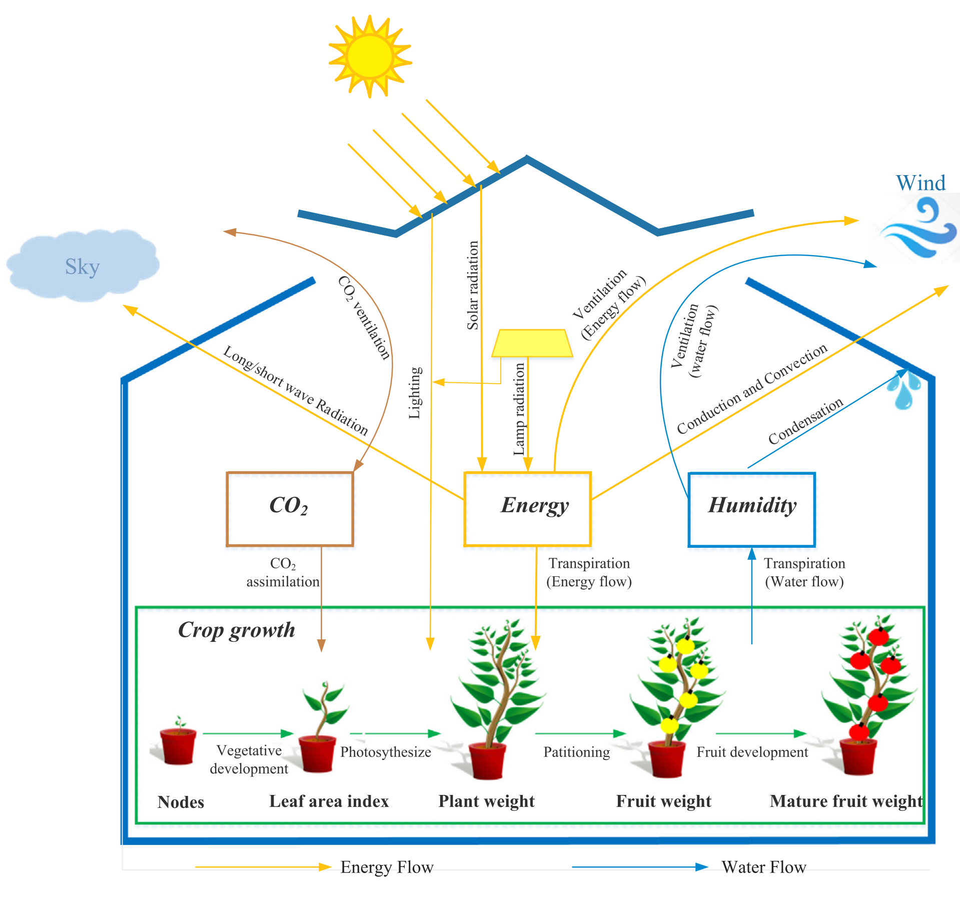

Fig. 1. Overview of the integrated modeling framework.

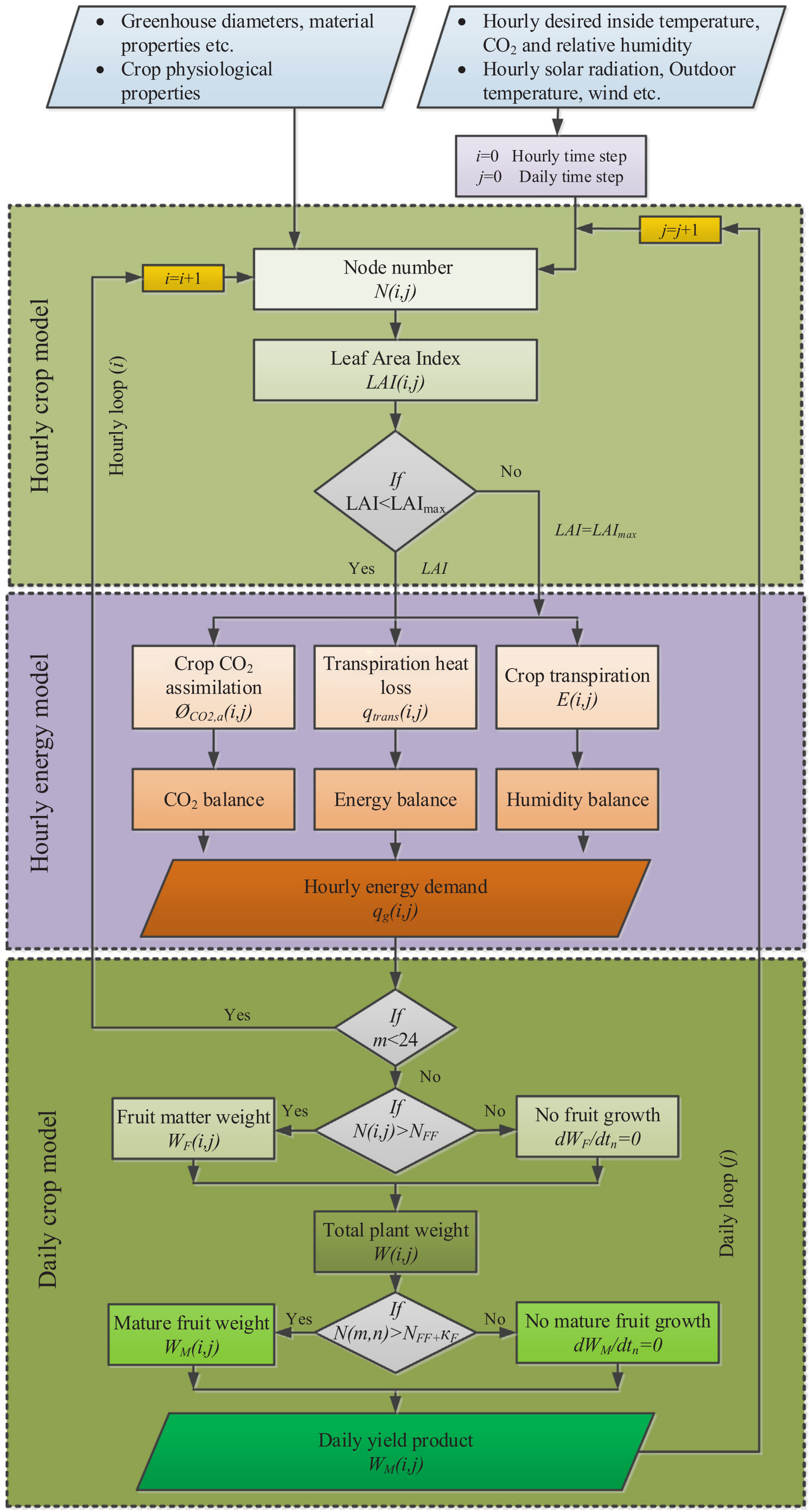

Fig. 2. Schematic algorithm for developing the integrated framework of greenhouse energy-crop growth.

shows that models without crop growth feedback overestimate transpiration loss in the beginning of crop planting and underestimate it during maximum LAI values. On the other hand, crop model feedback is taken into account in the integrated model. The inclusion of feedback from crop growth in the integrated model shows the importance of including seasonality in modeling a greenhouse.

Fig. 6 shows the effect of including feedback from the crop growth model on the greenhouse monthly and daily energy demand. The metric performance of both, the integrated and the standalone energy model are worse for daily time steps than in the monthly analysis. The only

Table 2
Physical features and operating set points of Agroscope greenhouse.

Parameter	Dimension	Value
Greenhouse floor area	m^2	359
Greenhouse height	m	5
Greenhouse surface area	m^2	468
Number of windows per m^2	–	0.078
Length of the window	m	2
Plant density	number of plants m^{-2} ground	3.47
Roof slope	degree	45
Day/night temperature set point	°C	20/16
CO_2 concentration set point	ppm	500
Humidity set point	%	70–90

exception is PBIAS, which suggests that the underestimation in the daily analysis is lower, compared to the monthly one.

However, in both cases, the integrated model performs better than the standalone energy model without crop feedback. Particularly, during warm days of the year (from day 180 on in Fig. 6-b) which coincide with high levels of Leaf Area Index (LAI) and solar radiation, the differences between two models are more pronounced. Therefore, the consideration of crop feedback improves model performance regardless of the time resolution.

Fig. 7 shows the observed and simulated data for fruit dry weight. The model shows a very high determination for the R^2 of 0.96 and a less positive result for the RRMSE with 0.23. Overall the model appears to underestimate crop yield (*PBIAS* = 0.18). These results are very similar to the ones from the validation dataset of Jones et al. [50], as illustrated in Fig. S.4. Nevertheless, the comparison of Fig. 7 and Fig. S.4c shows that the crop yield model of the present work has estimated fruit dry weight of the Agroscope greenhouse with higher accuracy in comparison to the Lake City greenhouse in [50]. This is likely because of the use of more precise hourly data for the environmental conditions of the Agroscope greenhouse. In contrast, the climate data used for simulating the fruit dry weight of Lake City greenhouse was based on daily averages due to a lack of more detailed data. This illustrates the importance of high resolution climate data availability.

To investigate the general performance of the integrated model, three indices are defined and results are compared in Table 3. *Index i* indicates the amount of heating energy that is consumed to provide favorable conditions in the Agroscope greenhouse and is used to analyze the energy demand performance of the integrated model. *Index ii* evaluates total crop growth performance of the integrated model. *Index iii* shows the amount of energy which is needed to produce one unit of yield. Although indices *i* and *ii* are useful to investigate the performance of energy and crop growth model separately, specific energy (index *iii*) is a more meaningful measure to compare the tradeoffs between energy and crop growth. Observed and simulated values of these indices and their relative errors are compared in the Table 2. The most important reason of errors is that the integrated model was not calibrated to the specific greenhouse. Although calibration could reduce the relative errors, it was our intention to present the raw output data to evaluate the model performance as a predictive tool in situations where no measurements are available.

Further evaluations of the individual model parts can be found in the Supporting Information Section 3.

3.2. Analysis of renewable energy integration

The appropriate use of renewable energy sources has a substantial potential to reduce greenhouse energy demand. Storage of solar energy during day and releasing it during night has been found to be one of the most cost-effective methods of renewable energy utilization [5,79,80]. To illustrate the application of the model in conjunction with renewable energy use, we model the use of phase change materials (PCM) [79,81,82] for the Agroscope greenhouse. Using the previous model, we assume that a calcium chloride hexahydrate ($CaCl_2 \cdot 6H_2O$) element of 4 cm thickness is used as a PCM element on the north-facing wall of the greenhouse. As seen in Fig. 8-a, temperature set points for tomato crop are 24 °C and 16 °C for day and night, respectively. Without the PCM element and without an active heating system, the inside temperature comes close to the outside temperature at night. With the use of the PCM element, however, indoor temperature remains at about 12 °C without energy input and, therefore, considerably above the outside temperature. This translates to considerable energy savings, as illustrated in Fig. 8-b. The cumulated heat demand throughout the day (dotted lines) is almost half for the PCM case, compared to the situation without PCM.

Fig. 9 illustrates the effect of thermal storage on energy demand for an entire crop season. The energy savings are particularly high during the cold months of the year, due to longer nights and colder outdoor temperatures. On average, the use of PCM reduces annual energy consumption by 15%. As the benefits from integrating renewable or sustainable energies depend on a number of factors, the model can be a helpful tool for planers to evaluate the economic, energetic, and environmental benefit of greenhouse design. Further advanced renewable energy strategies will be investigated for greenhouses in an upcoming paper.

3.3. Sensitivity analysis

3.3.1. Effects of greenhouse temperature set point

Literature review shows that growers use different temperature set points in the greenhouse [30,52,83,84]. Capacity limitations may be one reason, such as disability of energy supply system to provide higher temperature, lack of sufficient ventilation system to remove accumulated heating and extreme climate conditions. To evaluate the impacts of greenhouse temperature on both energy demand and crop yield, four temperature scenarios (Fig. 10) are simulated with integrated model of this work. Therefore, other inputs of the integrated model, such as CO_2 concentration, lighting, solar radiation and other climate conditions are the same as in the Agroscope reference greenhouse and only temperature set points are changed.

In scenario A, day and night temperature set points are both decreased by 2 °C in comparison to the base case, to 18 °C and 14 °C, respectively. The result shows that the energy consumption (*Index i*) will be decreased by 30% and yield production (*Index ii*) will be decreased by 21%. 11% decrease in specific energy (*Index iii*) shows that this scenario can be applicable for greenhouse provided that less energy consumption is more important than more yield production. In scenario B, both day and night temperatures are 18 °C. In comparison with the base case, day temperature set point is dropped by 2 °C but night temperature set point is increased by 2 °C. Fig. 10 shows 4% decrease in

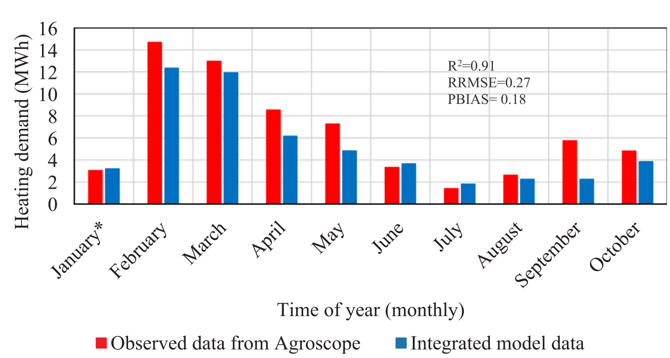

Fig. 3. Observed (red) and simulated (blue) monthly heating demand of the greenhouse. * The last 6 days of this month is presented in the figure (For interpretation of the references to color in this figure, the reader is referred to the web version of this article).

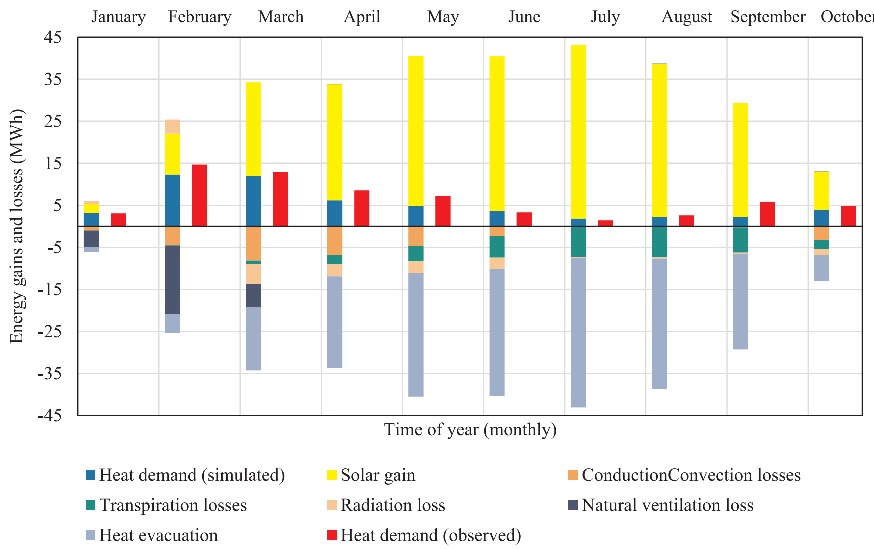

Fig. 4. Monthly heat demand, heat gain and heat losses in the greenhouse.

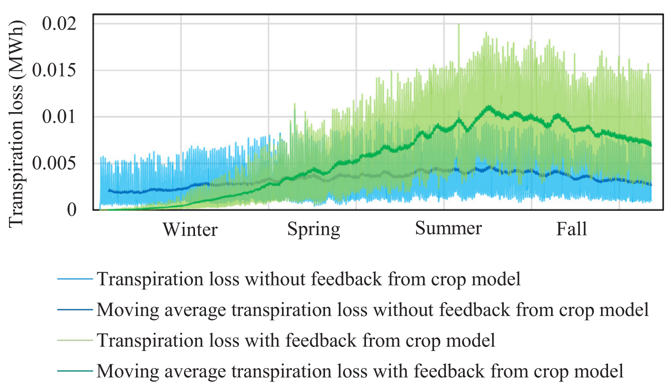

Fig. 5. Transpiration loss with and without crop growth model feedback.

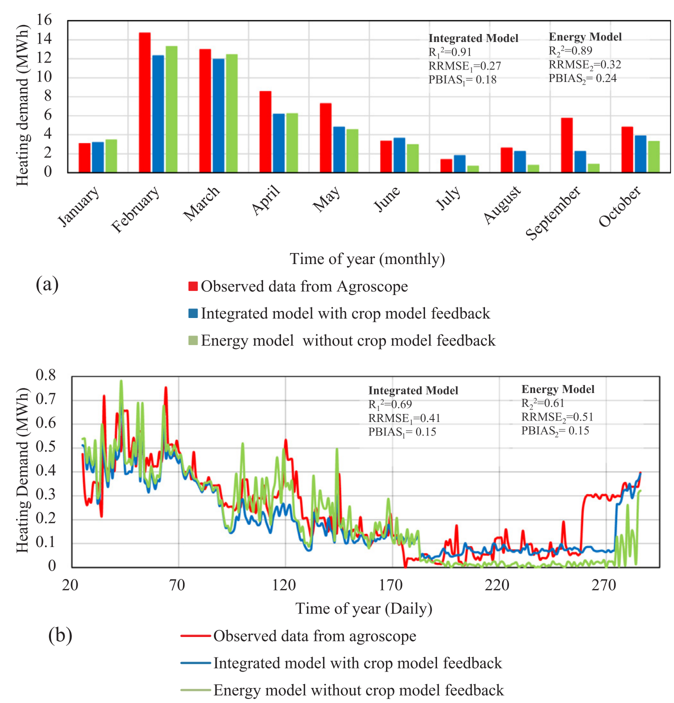

Fig. 6. Comparison of monthly (a) and daily (b) energy demand estimated by the integrated model and the energy model without crop growth feedback. Indices subscripts 1 and 2 denote the correlation between the integrated model results and the observed data and between energy model without crop growth feedback results and the observed data, respectively.

energy consumption, 1.5% decrease in yield production and 3% decrease in specific energy. Although these values are small in comparison with first scenario, in large greenhouses these differences can add up to significant absolute energy savings. The comparison of scenario A with B depicts the effect of night temperature set point: with a 4 °C increase in night temperature set point 25% more energy is consumed and 18% more yield is produced.

To evaluate the effect of day temperature, scenario C analyses the increase of day temperature set point by 4 °C and the same night temperature as base case. In this scenario, energy consumption (*Index i)* and yield production (*Index ii*) are increased by 20% and 25%, respectively. It confirms that increasing day temperature is more beneficial in comparison to night temperature in both aspects of less energy consumption and more yield production. Another conclusion from scenario C is the reduction of specific energy (*Index iii*) whiles both indices *i* and *ii* are increased. It shows that day and night temperature set points of scenario C (24/16 °C) can be applicable for greenhouses which more yield production has higher preference than less energy consumption.

For analyzing the response of the integrated model to high temperatures, scenario D considers 28 °C and 22 °C as day and night temperature set points. As predicted, energy consumption is increased by 40% which is a considerable amount. However, in spite of increasing temperature, yield production is decreased by 23%. This result is in contrast with scenario C. The reason is that day temperatures slightly above 25 °C cause to start fruit abortion. Previous works [84] confirm result of scenario D which 25 °C is the critical temperature for tomato yield production. Rainwater et al. [85] found a yield decrease of 22–51% as a result of crop growth in hot greenhouses (average temperature of 34 °C) while scenario D of this work predicts a 23% yield decrease in 28 °C.

To conclude, day and night temperature set points have a different influence on greenhouse energy consumption and yield production. The developed integrated model in this work can be used as a powerful decision support tool for growers and decision makers to choose the optimum diurnal temperature according to their preferences for consuming less energy, producing more yield, causing less environmental impacts, etc.

3.3.2. *Effects of CO_2 concentration set point*

Fig. 11 represents the effects of different CO_2 concentration set

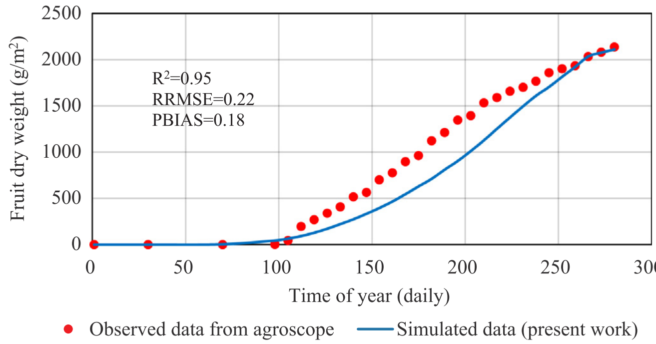

Fig. 7. The observed and simulated greenhouse yield.

Table 3
observed and simulated data for greenhouse total heating energy consumption (Index i), total dry basis yield (index ii) and consumed heating energy for 1 kg of produced yield (index iii).

Index	Dimension	Value		Relative error %
		Observed	Simulated	
Total annual heating energy (Index *i*)	kWh	64,318	52,144	− 19%
Total annual dry basis yield (Index *ii*)	kg	781	756	− 3%
Specific energy (Index *iii*[a])	kWh/kg	82	69	− 16%

[a] Index *iii* = Heating energy demand / Yield.

points on greenhouse yield production. Energy consumption of the CO_2 enrichment system was not considered. If fossil or biomass fuels are used for greenhouse heating and cooling, CO_2 rich flue gas comes "for free" and can be used to increase greenhouse CO_2 concentrations.

For analyzing the effects of CO_2 on crop yield production, four CO_2 concentration set points are applied to the integrated model based on experimental greenhouses [49,86,87]. Other inputs of the integrated model such as temperature set points, lighting, solar radiation and other climate conditions are kept the same as in the Agroscope reference greenhouse. In scenario A, CO_2 concentration set point is 250 ppm. This scenario happens when there is not any CO_2 enrichment and greenhouse air CO_2 concentration drops to 250 ppm due to crop CO_2 assimilation. The results of scenario A show that greenhouse yield is reduced by 24% in comparison with the base case (500 ppm). It confirms the importance of CO_2 enrichment to keep greenhouse air CO_2 concentration at the same level as fresh air CO_2 concentration as in Scenario B. The increase of yield production resulted by increasing CO_2 concentration to more than 650 ppm in scenarios C and D is limited. Therefore, the marginal benefit of increasing CO_2 set point on yield production is larger at low CO_2 concentrations than higher concentrations. The optimum CO_2 set point for the Agroscope greenhouse was 650 ppm based on our model.

3.3.3. Effects of artificial lighting

Increasing artificial lighting not only increases photosynthetic photon flux density but also heats up the greenhouse air. However, it consumes electrical energy. To extend the hours of natural daylight or to provide a night interruption to maintain the plants on long-day conditions, artificial lighting is necessary. In this work, four levels of artificial lighting are analyzed. For adding the artificial lighting, metal halide lamps are simulated during night (111.4 W m^{-2} or 9000 lx). The effect of artificial lighting on crop growth is simulated by net radiation at crop level during night time (See Eq. S.14). Amount of heat generation and electrical energy consumption by lamps are calculated by Eqs. (S.3) and (S.4). When artificial lighting is used in the greenhouse, energy consumption (*index i*) considers the effects of both lamps heat generation and equivalent thermal energy of electricity consumption.

Fig. 12 shows that by increasing artificial lighting both energy consumption (*Index i*) and yield production (*Index ii*) are increased. However, specific energy (*Index iii*) is increased in scenarios A and B and then decreased in scenarios C and D. It confirms that more artificial lighting has a higher effect on increasing yield production than energy consumption. Another conclusion is that for having a beneficial artificial lighting, at least 2000 lx (scenario C) should be added during night time, based on result of our work.

4. Discussion

For the aim of greenhouse energy systems design and operation optimization, the presented integrated framework has several advantages compared to the existing literature. For example, in comparison to the models of Van Beveren et al. and Chen et al. [30,33], 1) It considers the effects of plant node development and leaf area index expansion on transpiration heat loss. 2) The model analyzes different heat loss drivers (Fig. 4) in the greenhouse, which enables to identify the most important sources of heat loss in different seasons. 3) It calculates greenhouse energy demand, and can therefore be coupled flexibly with various energy supply technologies.

There are some models in the literature which take into account the effects of greenhouse air condition on yield production [12,63]. The advantage of the integrated model in this work is the investigation of mutual effects of greenhouse energy demand and crop growth. This means that our integrated model does not only consider the impacts of greenhouse air condition on yield production, but also it would be able to investigate the effects of crop growth and yield production on greenhouse energy demand. In addition, the model is able to investigate the impact of retrofitting conventional greenhouses with strategies for the integration of renewable energy resources.

Sensitivity analysis results showed that the current model can be used to study the possible effects of different environmental control strategies over practical ranges of temperature set points, CO_2 set points and lighting. Elings et al. [88] found 16% energy saving by reducing the temperature set point by 2 °C. The integrated model showed a 30% decrease in energy consumption, as a result of 4 °C decrease in set points (Fig. 10, scenario A). Jones et al. [49] found reductions in fruit yield of 30% when temperature set points decreased from 28/16 °C day/night to 20/12 °C, which means 2.5% less yield per 1 °C lower temperature set point. The integrated model of the present work calculates 3.1% less yield production for 1 °C lower temperature set point.

Based on results of CO_2 set point sensitivity analysis of this work, optimal CO_2 concentration is in the range of 600–800 ppm while Mortensen [86] recommended a CO_2 concentration of 700–900 ppm. Similar to the findings of this work (Fig. 11), Nederhoff [87] showed that the effect of CO_2 concentration on plant growth is higher at low levels (200–340 ppm) than at high levels (500–700 ppm). Jones et al. [49] found 18% increase in yield production when CO_2 was increased from 350 to 950 ppm with temperatures of 28/16. This work shows 22% increase in yield production when CO_2 is increased from 350 to 800 ppm with day/night temperatures of 20/16 °C. Marcelis et al. [74] and Tremblay et al. [89] demonstrated a 0.7–1% yield increase for 1% light increase for fruit vegetables under temperate greenhouse climate conditions, in accordance with the findings of this paper (Fig. 12).

As explained in Section 2.3, greenhouse physical properties and local climate condition are model inputs. Therefore, it is possible to use the model for wide variety of greenhouses in different climate conditions around the world. The model is able to evaluate energy consumption and yield production according to greenhouse type and local climate condition. Application of the model in different climate regions and investigating the effective physical properties in each region is the aim of authors' future publication.

Additional insights of the results include: i) the need for considering the performance of both energy demand and crop growth model, ii) the

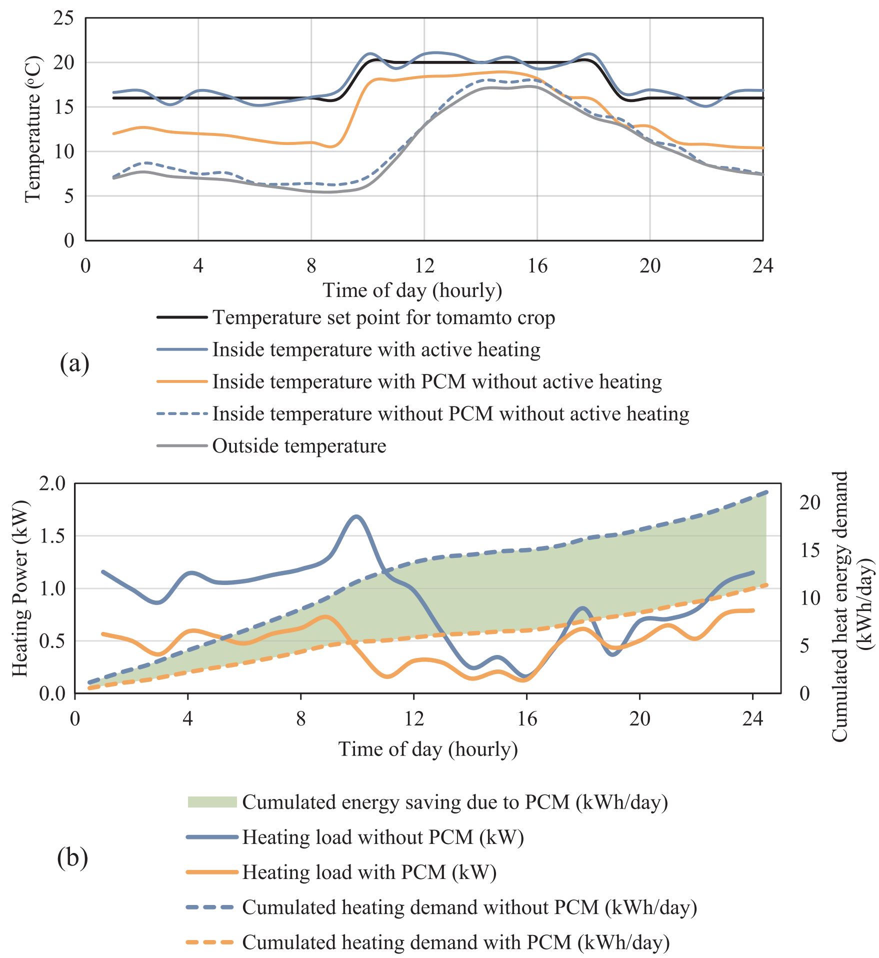

Fig. 8. a) Modeled diurnal temperature development with and without phase change material (PCM) for the Agroscope greenhouse (Switzerland, March 29). b) Hourly heating load and cumulated heating demand.

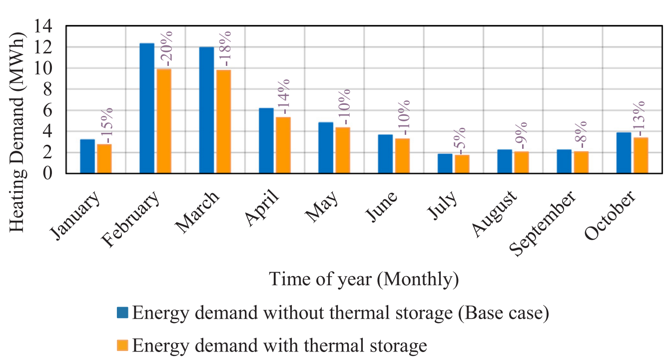

Fig. 9. Monthly energy demand of the Agroscope greenhouse with and without PCM storage. Percentages refer to the energy savings of the PCM case, compared to the case without PCM.

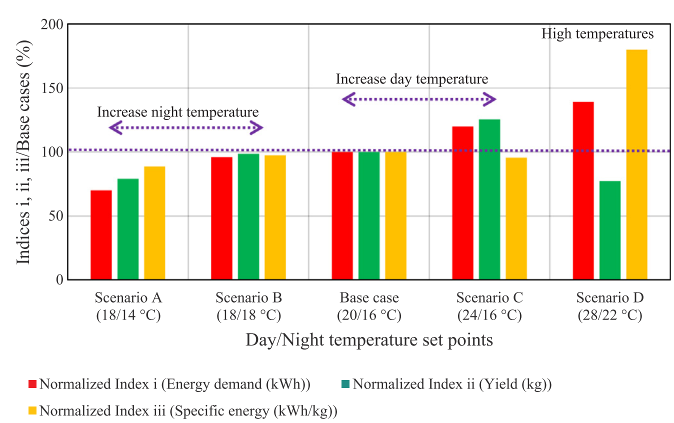

Fig. 10. Relative effect of day/night temperatures variations on three indices of greenhouse performance. Base case is 100%. The numbers in parentheses show the day and night temperatures. In all scenarios, CO_2 concentration is 500 ppm without artificial lighting.

effect of vegetative crop growth on transpiration and greenhouse energy loss particularly when leaf area index is at its maximum value, iii) the potential advantages of a dynamic approach to investigate simultaneous impacts of greenhouse energy demand and crop production during different seasons.

5. Conclusions

In this article, an integrated modeling framework to investigate the direct and indirect interactions of greenhouse energy demand and crop yield is proposed. The main goal was to understand the dynamic behavior of greenhouse climate condition and crop growth as much as possible to investigate the real performance of the greenhouse by means of an integrated model. This model is able to simultaneously consider the effect of changing climate conditions and physical parameters on energy consumption and crop yield.

The overall performance of the integrated model is validated by data collected for one full tomato growing period from the Agroscope research institute in Switzerland. There was good agreement with the

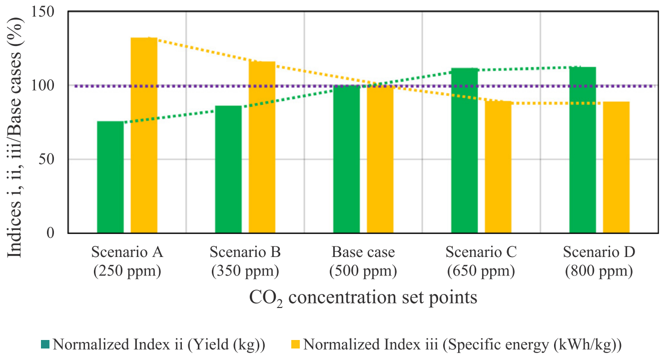

Fig. 11. Relative effect of CO_2 concentration on three indices of greenhouse performance. Base case is 100%. In all scenarios, day/night temperatures are 20/16 °C without artificial lighting.

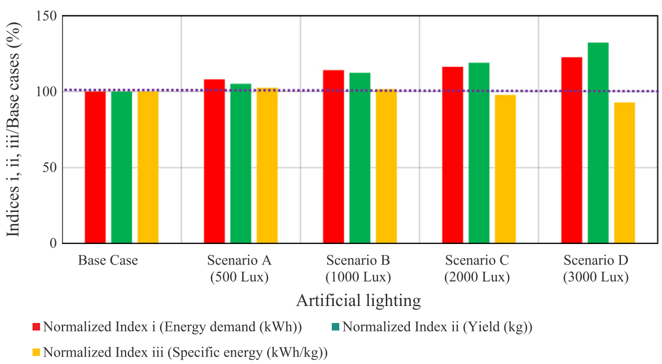

Fig. 12. Relative effect of artificial lighting on three indices of greenhouse performance. Base case is 100%. In all scenarios, day/night temperatures are 20/16 and CO_2 concentration is 500 ppm. The electrical energy of lamps is added to greenhouse thermal energy by use of its exergy efficiency explained in Eq. (S.4).

results of the integrated model and the observed dataset. The model was found to have high predictive power with a tendency to underestimate both energy demand and crop yield results, which is illustrated by the correlation metrics: for energy demand R^2 is 0.91, RRMSE is 0.27 and PBIAS is 0.18. The values of R^2, RRMSE and PBIAS for crop yield are 0.95, 0.22 and 0.18, respectively. The temporally differentiated analysis of energy gains and losses showed that dominant energy loss mechanisms varied during different seasons and crop growth periods. One key advantage of the integrated model is that it points to the main drivers of greenhouse energy losses and yield implications, identifying hotspots. Specifying main energy loss mechanisms and understanding the interlinkages with crop yield can be used for a better design and operation of greenhouses. Furthermore, we illustrated how the model's capacity to evaluate strategies for integrating renewable energy sources on the example of phase change materials.

The sensitivity analysis of day/night temperature, CO_2 concentration and artificial lighting showed that with lower yields, there is a potential for lower specific energy consumption (per unit of yield). On the other hand, if higher yield rates are desired, there will be increasing energy requirements. For instance, decreasing the greenhouse day and night temperatures by 2 °C will decrease energy consumption by 30%, but will provide only 79% of the baseline greenhouse yield.

The main aim of this study was to develop and validate an integrated model. It can be used as a decision support tool for constructing new greenhouses according to their appropriate climate condition or retrofitting existing greenhouses. The consideration of dynamic effects and the high temporal resolution allow a detailed assessment to use local renewable energy sources as sustainable choices. Finally and primarily, the present integrated model can help growers in improving the operation of greenhouses. This includes determining favorable bounds and set points of temperature, CO_2 concentration and humidity to achieve optimum results for energy consumption, yield, environmental impacts, economic benefit, etc. In future research, an optimization framework will be combined with the integrated model to achieve the highest possible performance of a greenhouse according to the preferences of growers and other decision makers (e.g. agricultural policy makers, sustainable labeling initiatives). Furthermore, the model results will be coupled with life cycle assessment (LCA) data to perform an environmental assessment of greenhouses. This will allow one to compare measures, such as increased CO_2 concentration, against an increased heat energy input or different heat sources. Also, the consideration of crops other than tomatoes in different climate regions around the world will be done in future research to provide a comprehensive tool.

Acknowledgement

This research was supported by the Swiss Federal Institute of Technology in Zurich (ETH Zurich) and Sharif University of Technology [grant number 1408690]. The authors would like to thank Gilli Céline from Agroscope, Switzerland, Jochen Hemming and Jan Bontsema from Wageningen Greenhouse Horticulture, for providing the greenhouse climate data needed to validate the model and Christie Walker for proofreading the manuscript.

Appendix A. Supporting information

Supplementary data associated with this article can be found in the online version at doi:10.1016/j.rser.2018.06.046.

References

[1] Canakci M, Yasemin Emekli N, Bilgin S, Caglayan N. Heating requirement and its costs in greenhouse structures: a case study for Mediterranean region of Turkey. Renew Sustain Energy Rev 2013;24:483–90. https://doi.org/10.1016/j.rser.2013.03.026.
[2] Yildirim N, Bilir L. Evaluation of a hybrid system for a nearly zero energy greenhouse. Energy Convers Manag 2017;148(Supplement C):1278–90. https://doi.org/10.1016/j.enconman.2017.06.068.
[3] Wang T, et al. Integration of solar technology to modern greenhouse in China: current status, challenges and prospect. Renew Sustain Energy Rev 2017;70(Supplement C):1178–88. https://doi.org/10.1016/j.rser.2016.12.020.
[4] Esen M, Yuksel T. Experimental evaluation of using various renewable energy sources for heating a greenhouse. Energy Build 2013;65:340–51. https://doi.org/10.1016/j.enbuild.2013.06.018.
[5] Cuce E, Harjunowibowo D, Cuce PM. Renewable and sustainable energy saving strategies for greenhouse systems: a comprehensive review. Renew Sustain Energy Rev 2016;64(Supplement C):34–59. https://doi.org/10.1016/j.rser.2016.05.077.
[6] Chen J, Zhao J, Xu F, Hu H, Ai Q, Yang J. Modeling of energy demand in the greenhouse using PSO-GA hybrid algorithms. Math Probl Eng 2015;2015:6. https://doi.org/10.1155/2015/871075.
[7] Van Beveren PJM, Bontsema J, Van Straten G, Van Henten EJ. Optimal control of greenhouse climate using minimal energy and grower defined bounds. Appl Energy 2015;159:509–19. https://doi.org/10.1016/j.apenergy.2015.09.012.
[8] Bartzas G, Zaharaki D, Komnitsas K. Life cycle assessment of open field and greenhouse cultivation of lettuce and barley. Inform Process Agric 2015;2(3–4):191–207. https://doi.org/10.1016/j.inpa.2015.10.001.
[9] Dias GM, Ayer NW, Khosla S, Van Acker R, Young SB, Whitney S, Hendricks P. Life cycle perspectives on the sustainability of Ontario greenhouse tomato production: benchmarking and improvement opportunities. J Clean Prod 2017;140(Part 2):831–9. https://doi.org/10.1016/j.jclepro.2016.06.039.
[10] Zhang H, Burr J, Zhao F. A comparative life cycle assessment (LCA) of lighting technologies for greenhouse crop production. J Clean Prod 2017;140(Part 2):705–13. https://doi.org/10.1016/j.jclepro.2016.01.014.
[11] Bojacá CR, Wyckhuys KAG, Schrevens E. Life cycle assessment of Colombian greenhouse tomato production based on farmer-level survey data. J Clean Prod 2014;69(Supplement C):26–33. https://doi.org/10.1016/j.jclepro.2014.01.078.
[12] Vanthoor BHE, Van Henten EJ, Stanghellini C, De Visser PHB. A methodology for model-based greenhouse design: part 3, sensitivity analysis of a combined greenhouse climate-crop yield model. Biosyst Eng 2011;110(4):396–412. https://doi.org/10.1016/j.biosystemseng.2011.08.006.
[13] Coomans M, Allaerts K, Wittemans L, Pinxteren D. Monitoring and energetic performance of two similar semi-closed greenhouse ventilation systems. Energy Convers Manag 2013;76(Supplement C):128–36. https://doi.org/10.1016/j.

enconman.2013.07.028.
[14] Euoropean Commission. Energy optimisation in European greenhouses. 2009. 〈https://cordis.europa.eu/project/rcn/74800_en.html〉.
[15] Gołaszewski J, et al. State of the art on energy efficiency in agriculture. Country data on energy consumption in different agroproduction sectors in the European countries. Agriculture and Energy Efficiency. 2012http://www.agree.aua.gr/files/agree_state.pdf.
[16] Natural Resources Institute Finland. Energy consumption by greenhouses decreasing – renewables account for 40% of heat energy. 〈https://www.luke.fi/en/news/energy-consumption-by-greenhouses-decreasing-renewables-account-for-40-of-heat-energy/〉; 2015.
[17] Campiotti C, Viola C, Alonzo G, Bibbiani C, Giagnacovo G, Scoccianti M, Tumminelli G. Sustainable greenhouse horticulture in Europe. J Sustain Energy 2012;3(3). [DOI: https://arpi.unipi.it/retrieve/handle/11568/788029/92641/v3-n3-7.pdf].
[18] Hassanien RHE, Li M, Dong Lin W. Advanced applications of solar energy in agricultural greenhouses. Renew Sustain Energy Rev 2016;54:989–1001. https://doi.org/10.1016/j.rser.2015.10.095.
[19] Bayrakcı AG, Koçar G. Utilization of renewable energies in Turkey's agriculture. Renew Sustain Energy Rev 2012;16(1):618–33. https://doi.org/10.1016/j.rser.2011.08.027.
[20] Vadiee A, Martin V. Energy analysis and thermoeconomic assessment of the closed greenhouse – the largest commercial solar building. Appl Energy 2013;102:1256–66. https://doi.org/10.1016/j.apenergy.2012.06.051.
[21] Çakır U, Şahin E. Using solar greenhouses in cold climates and evaluating optimum type according to sizing, position and location: a case study. Comput Electron Agric 2015;117:245–57. https://doi.org/10.1016/j.compag.2015.08.005.
[22] He X, Wang J, Guo S, Zhang J, Wei B, Sun J, Shu S. Ventilation optimization of solar greenhouse with removable back walls based on CFD. Comput Electron Agric 2017. https://doi.org/10.1016/j.compag.2017.10.001〈https://doi.org/10.1016/j.compag.2017.10.001〉.
[23] Lu W, Zhang Y, Fang H, Ke X, Yang Q. Modelling and experimental verification of the thermal performance of an active solar heat storage-release system in a Chinese solar greenhouse. Biosyst Eng 2017;160:12–24. https://doi.org/10.1016/j.biosystemseng.2017.05.006.
[24] Groener B, Knopp N, Korgan K, Perry R, Romero J, Smith K, Stainback A, Strzelczyk A, Henriques J. Preliminary design of a dow-cost greenhouse with open source control systems. Procedia Eng 2015;107:470–9. https://doi.org/10.1016/j.proeng.2015.06.105.
[25] Pack, M. and Mehta, K. Design of affordable greenhouses for East Africa. In: Proceedings of IEEE global humanitarian technology conference; 2012. Seattle, Washington: IEEE. 〈http://sites.psu.edu/hese/2016/03/16/1607/〉.
[26] Joudi KA, Farhan AA. A dynamic model and an experimental study for the internal air and soil temperatures in an innovative greenhouse. Energy Convers Manag 2015;91:76–82. https://doi.org/10.1016/j.enconman.2014.11.052.
[27] Singh G, Singh PP, Lubana PPS, Singh KG. Formulation and validation of a mathematical model of the microclimate of a greenhouse. Renew Energy 2006;31(10):1541–60. https://doi.org/10.1016/j.renene.2005.07.011.
[28] Cabello T, Gallego JR, Fernandez FJ, Gamez M, Vila E, Del Pino M, E H-S. Biological control strategies for the South American tomato moth (Lepidoptera: gelechiidae) in greenhouse tomatoes. J Econ Entomo 2012;105(6):20〈https://www.ncbi.nlm.nih.gov/pubmed/23356074〉.
[29] Berdegué JA, Fuentealba R. Latin America: the state of smallholders in agriculture, In: Proceedings of IFAD conference on new directions for smallholder agriculture, IFAD: Rome; 2011.
[30] Van Beveren PJM, Bontsema J, Van Straten G, Van Henten EJ. Minimal heating and cooling in a modern rose greenhouse. Appl Energy 2015;137:97–109. https://doi.org/10.1016/j.apenergy.2014.09.083.
[31] Cuce E, Harjunowibowo D, Cuce PM. Renewable and sustainable energy saving strategies for greenhouse systems: a comprehensive review. Renew Sustain Energy Rev 2016;64:34–59. https://doi.org/10.1016/j.rser.2016.05.077.
[32] Marucci A, Zambon I, Colantoni A, Monarca D. A combination of agricultural and energy purposes: evaluation of a prototype of photovoltaic greenhouse tunnel. Renew Sustain Energy Rev 2018;82:1178–86. https://doi.org/10.1016/j.rser.2017.09.029.
[33] Chen J, Yang J, Zhao J, Xu F, Shen Z, Zhang L. Energy demand forecasting of the greenhouses using nonlinear models based on model optimized prediction method. Neurocomputing 2016;174(Part B):1087–100. https://doi.org/10.1016/j.neucom.2015.09.105.
[34] Walker JN. Predicting temperatures in ventilated greenhouses. Trans ASAE 1965;8(3). https://doi.org/10.13031/2013.40545.
[35] Businger JA. The glasshouse (greenhouse) climate. In: Van Wijk WR, editor. Physics of Plant Environment. Amsterdam: North-Holland; 1963. p. 277–318.
[36] Takakura T, Jordan KA, Boyd LL. Dynamic simulation of plant growth and environment in the greenhouse. Trans ASAE 1971;14(5). https://doi.org/10.13031/2013.38432.
[37] Van Bavel CHM, Damagnez J, Sadler EJ. The fluid-roof solar greenhouse: energy budget analysis by simulation. Agric Meteorol 1981;23:61–76. https://doi.org/10.1016/0002-1571(81)90091-1.
[38] Bot GPA. Greenhouse climate: from physical processes to a dynamic model, Bot: Wageningen; 1983. 〈http://edepot.wur.nl/188427〉.
[39] Deltour J, de Halleux D, Nijskens J, Coutisse S, Nisen A. Dynamic Modelling of Heat and Mass Transfer in Greenhouses. Leuven, Belgium: International Society for Horticultural Science (ISHS); 1985. https://doi.org/10.17660/ActaHortic.1985.174.14.
[40] Tiwari GN, Sharma PK, Goyal RK, Sutar RF. Estimation of an efficiency factor for a greenhouse: a numerical and experimental study. Energy Build 1998;28(3):241–50. https://doi.org/10.1016/S0378-7788(97)00062-5.
[41] Chou SK, Chua KJ, Ho JC, Ooi CL. On the study of an energy-efficient greenhouse for heating, cooling and dehumidification applications. Appl Energy 2004;77(4):355–73. https://doi.org/10.1016/S0306-2619(03)00157-0.
[42] Sethi VP. On the selection of shape and orientation of a greenhouse: thermal modeling and experimental validation. Sol Energy 2009;83(1):21–38. https://doi.org/10.1016/j.solener.2008.05.018.
[43] Vanthoor BHE, Stanghellini C, Van Henten EJ, De Visser PHB. A methodology for model-based greenhouse design: part 1, a greenhouse climate model for a broad range of designs and climates. Biosyst Eng 2011;110(4):363–77. https://doi.org/10.1016/j.biosystemseng.2011.06.001.
[44] Vanthoor BHE, De Visser PHB, Stanghellini C, Van Henten EJ. A methodology for model-based greenhouse design: part 2, description and validation of a tomato yield model. Biosyst Eng 2011;110(4):378–95. https://doi.org/10.1016/j.biosystemseng.2011.08.005.
[45] Heuvelink E. Dry matter production in a tomato crop: measurements and simulation. Ann Bot 1995;75(4):369–79. https://doi.org/10.1006/anbo.1995.1035.
[46] Heuvelink, E., Tomato growth and yield: quantitative analysis and synthesis Unpublished PhD thesis, Wageningen Agricultural University, Wageningen, The Netherlands; 1996. p. 326.
[47] HEUVELINK E. Evaluation of a dynamic simulation model for tomato crop growth and development. Ann Bot 1999;83:413–22.
[48] Abreu P, Meneses JF, Gary C. TOMPOUSSE, a model of yield prediction for tomato crops: calibration study for unheated plastic greenhouses. Acta Hort. (ISHS) 2000;519:141–50.
[49] Jones JW, Dayan E, Allen LH, Keulen HV, Challa H. A dynamic tomato growth and yield model (TOMGRO). Trans ASAE 1991;34(2):0663–72. https://doi.org/10.13031/2013.31715.
[50] Jones JW, Kenig A, Vallejos CE. Reduced state-variable tomato growth model. Trans ASAE 1999;42(1):255–65. https://doi.org/10.13031/2013.13203.
[51] Kenig A, Jones JW. TOMGRO V3.0: A dynamic model of tomato growth and yield, Ch II-5. In Optimal Environmental Control for Indeterminate Greenhouse Crops, eds. I. Seginer, J.W. Jones, P. Gutman, and C.E. Vallejos. BARD Research Report No. IS-1995-91RC. Haifa, Isreal: Agricultural Engineering Dept., Technion; 1997.
[52] Ramirez A, Rodriguez F, Berenguel M, Heuvelink E. Calibration and validation of complex and simplified tomato growth models for control purposes in the Southeast of Spain. Acta Hort 2004;654(ISHS).
[53] Bertin N, Heuvelink E. Dry-matter production in a tomato crop: comparison of two simulation models. J Hortic Sci 1993;68(6):995–1011. https://doi.org/10.1080/00221589.1993.11516441.
[54] Bacci L, Battista P, Rapi B. Evaluation and adaptation of TOMGRO model to Italian tomato protected crops. NZ J Crop Hortic Sci 2012;40(2):115–26. https://doi.org/10.1080/01140671.2011.623706.
[55] Dimokas G, Kittas C, Tchamitchian M. Validation of a tomato crop simultor for mediterranean greenhouses. Leuven, Belgium: International Society for Horticultural Science (ISHS); 2008. https://doi.org/10.17660/ActaHortic.2008.797.34.
[56] Shamshiri R, Ahmad D, Zakaria A, Ismail WIW, Man HC, Yamin M. Evaluation of the reduced state-variable TOMGRO model using boundary data In: Proceedings of ASABE annual international meeting. https://doi.org/10.13031/aim.20162454205; 2016.
[57] Nederhoff EM, Vegter JG. Photosynthesis of stands of tomato, cucumber and sweet pepper measured in greenhouses under various CO_2-concentrations. Ann Bot 1993;73(4):353–61. https://doi.org/10.1006/anbo.1994.1044.
[58] De Zwart HF. Analyzing energy-saving potentials in greenhouse cultivation using a simulation model, Thesis Landbouwuniversiteit Wageningen; 1996.
[59] Kempkes FLK, Bakker JC, Van De Braak NJ. Control and modelling of vertical temperature distribution in greenhouse crops. Acta Hortic 1998;456:363–70. https://doi.org/10.17660/ActaHortic.1998.456.43.
[60] Sharma PK, Tiwari GN, Sorayan VPS. Temperature distribution in different zones of the micro-climate of a greenhouse: a dynamic model. Energy Convers Manag 1999;40(3):335–48. https://doi.org/10.1016/S0196-8904(98)00100-9.
[61] Wang S, Deltour J. An experimental model for leaf temperature of greenhouse-grown tomato. Acta Hortic 1999;491:101–6. https://doi.org/10.17660/ActaHortic.1999.491.13.
[62] Trigui M, Barrington S, Gauthier L. SE—structures and environment: a strategy for greenhouse climate control, part I: model development. J Agric Eng Res 2001;78(4):407–13. https://doi.org/10.1006/jaer.2000.0647.
[63] Trigui M, Barrington S, Gauthier L. SE—structures and environment: a strategy for greenhouse climate control, Part II: model validation. J Agric Eng Res 2001;79(1):99–105. https://doi.org/10.1006/jaer.2000.0648.
[64] Bontsema J, Hemming J, Stanghellini C, Visser PHBd, Henten Ev, Budding J, Rieswijk T, Nieboer S. On-line estimation of the transpiration in greenhouse horticulture. In: Proceedings of the 2nd IFAC international conference on modeling and design of control systems in agriculture. Osijek Croatia; 2007.
[65] Sethi VP, Sumathy K, Lee C, Pal DS. Thermal modeling aspects of solar greenhouse microclimate control: a review on heating technologies. Sol Energy 2013;96(Supplement C):56–82. https://doi.org/10.1016/j.solener.2013.06.034.
[66] Dayan E, van Keulen H, Jones JW, Zipori I, Shmuel D, Challa H. Development, calibration and validation of a greenhouse tomato growth model: I. Description of the model. Agric Syst 1993;43(2):145–63. https://doi.org/10.1016/0308-521X(93)90024-V.
[67] Dayan E, Van Keulen H, Jones JW, Zipori I, Shmuel D, Challa H. Development, calibration and validation of a greenhouse tomato growth model: ii. Field calibration and validation. Agric Syst 1993;43(2):165–83. https://doi.org/10.1016/0308-

521X(93)90025-W.

[68] Gary C, Barczi JF, Bertin N, Tchamitchian M. Simulation of individual organ growth and development on a tomato plant: a model and a user-friendly interface. Leuven, Belgium: International Society for Horticultural Science (ISHS); 1995. https://doi.org/10.17660/ActaHortic.1995.399.23.

[69] Gary C, Jones JW, Longuenesse JJ. Modelling daily changes in specific leaf area of tomato: the contribution of the leaf assimilate pool. Leuven, Belgium: International Society for Horticultural Science (ISHS); 1993. https://doi.org/10.17660/ActaHortic.1993.328.19.

[70] Kenig A, Jones JW. TOMGRO V3.0: a dynamic model of tomato growth and yield, Ch. II-5. in optimal environmental control for indeterminate greenhouse crops, I Seginer, JW Jones, P Gutman, and CE Vallejoseds. BARD Research Report No. IS-1995-91RC. Haifa, Israel: Agricultural Engineering Dept., Technion; 1997.

[71] Vallejos CE, Jones JW, Williams FW. High temperature tomato experiments, Ch. II-3. In Optimal Environmental Control for Indeterminate Greenhouse Crops, eds. I. Seginer, J. W. Jones, P. Gutman, and C. E. Vallejos. BARD Research Report No. IS-1995-91RC. Haifa, Israel: Agricultural Engineering Dept., Technion; 1997.

[72] Shamshiri R, Thorp KR, Razif Mahadi M, Zakaria A, Ismail WIW, Ahmad D, Che Man H. Adaptive management framework for evaluating and adjusting micro-climate parameters in tropical greenhouse crop production systems; 2017.

[73] Masters GM. Renewable and efficient electric power systems. Canada: John Wiley & Sons; 2004. p. 645.

[74] Marcelis LFM, Koning ANMD. Crop growth: Biomass partitioning in plants, in Greenhouse Climate Control: An Integrated Approach, 84-92, eds. J. C. Bakker, G. P. A. Bot, H. Challa, and N. J. Van de Braak; 1995.

[75] Moriasi DN, Arnold JG, Van Liew MW, Bingner RL, Harmel RD, Veith TL. Model evaluation guidelines for systematic quantification of accuracy in watershed Simulations. Trans ASABE 2007;50:885–900. https://doi.org/10.13031/2013.23153.

[76] Scherer L, Venkatesh A, Karuppiah R, Pfister S. Large-scale hydrological modeling for calculating water stress indices: implications of improved spatiotemporal resolution, surface-groundwater differentiation, and uncertainty characterization. Environ Sci Technol 2015;49(8):4971–9. https://doi.org/10.1021/acs.est.5b00429.

[77] Gupta HV, Sorooshian S, Yapo PO. Status of automatic calibration for hydrologic models: comparison with multilevel expert calibration. J Hydrol Eng 1999;4(2). https://doi.org/10.1061/(ASCE)1084-0699(1999)4:2(135)#sthash.caPnNIJ2.dpuf.

[78] Kobayashi K, Salam MU. Comparing simulated and measured values using mean squared deviation and its components research partly supported by core research for evolutional science and technology (CREST) of Japan Science and technology corp. (JST). Agron J 2000;92(2):345–52. https://doi.org/10.2134/agronj2000.922345x.

[79] Kooli S, Bouadila S, Lazaar M, Farhat A. The effect of nocturnal shutter on insulated greenhouse using a solar air heater with latent storage energy. Sol Energy 2015;115:217–28. https://doi.org/10.1016/j.solener.2015.02.041.

[80] Benli H, Durmuş A. Performance analysis of a latent heat storage system with phase change material for new designed solar collectors in greenhouse heating. Sol Energy 2009;83(12):2109–19. https://doi.org/10.1016/j.solener.2009.07.005.

[81] Boulard T, Razafinjohany E, Baille A, Jaffrin A, Fabre B. Performance of a greenhouse heating system with a phase change material. Agric For Meteorol 1990;52(3):303–18. https://doi.org/10.1016/0168-1923(90)90088-N.

[82] Berroug F, Lakhal EK, El Omari M, Faraji M, El Qarnia H. Thermal performance of a greenhouse with a phase change material north wall. Energy Build 2011;43(11):3027–35. https://doi.org/10.1016/j.enbuild.2011.07.020.

[83] Heuvelink E. Influence of day and night temperature on the growth of young tomato plants. Sci Hortic 1989;38(1):11–22. https://doi.org/10.1016/0304-4238(89)90015-0.

[84] Sato S, Peet MM, Thomas JF. Physiological factors limit fruit set of tomato (Lycopersicon esculentum Mill.) under chronic, mild heat stress. Plant, Cell Environ 2000;23(7):719–26. https://doi.org/10.1046/j.1365-3040.2000.00589.x.

[85] Rainwater DT, Gossetp DR, Millhollon EP, Hanna HY, Banks SW, Lucas MC. The relationship between yield and the antioxidant defense system in tomatoes grown under heat stress. Free Radic Res 1996;25(5):421–35. https://doi.org/10.3109/10715769609149065.

[86] Mortensen LM. Review: co_2 enrichment in greenhouses. Crop responses. Sci Hortic 1987;33(1):1–25. https://doi.org/10.1016/0304-4238(87)90028-8.

[87] Nederhoff EM, Vegter JG. Photosynthesis of stands of tomato, cucumber and sweet pepper measured in greenhouses under various CO_2-concentrations. Ann Bot 1994;73(4):353–61. https://doi.org/10.1006/anbo.1994.1044.

[88] Elings A, Kempkes FLK, Kaarsemaker RC, Ruijs MNA, van de Braak NJ, Dueck TA. The energy balance and energy saving measures in greenhouse tomato cultivation. Acta Hortic 2005;691:67–74. https://doi.org/10.17660/ActaHortic.2005.691.5.

[89] Tremblay N, Gosselin A. Effect of carbon dioxide enrichment and light. Hortic Technol 1998;8:3.